Rupture Status Classification of Intracranial Aneurysms Using Morphological Parameters

Research Seminar Talk

Prepared by

Niloy Roy

Email: niloy.roy@tu-ilmenau.de

M.Sc. In Research in Computer and Systems Engineering
Technische Universität Ilmenau

Winter 2023/24

TECHNISCHE UNIVERSITÄT ILMENAU

Outline

- What is an intracranial aneurysm ?
- Research gap and objective
- Methodology
- Results
- Limitations
- Future work
- References and acknowledgements

Intracranial Aneurysm

- Aneurysm: Dilations (e.g., bulge or ballooning) of a large blood-supplying vessel
- Approximately, 85% of aneurysms in the circle of Willis
- Mortality in rupture: 50%, morbidity : permanent deficits in 46% survivors
- Often no symptoms before rupture
- Rupture risk prediction of asymptomatic aneurysms is essential

Data source: References[3]

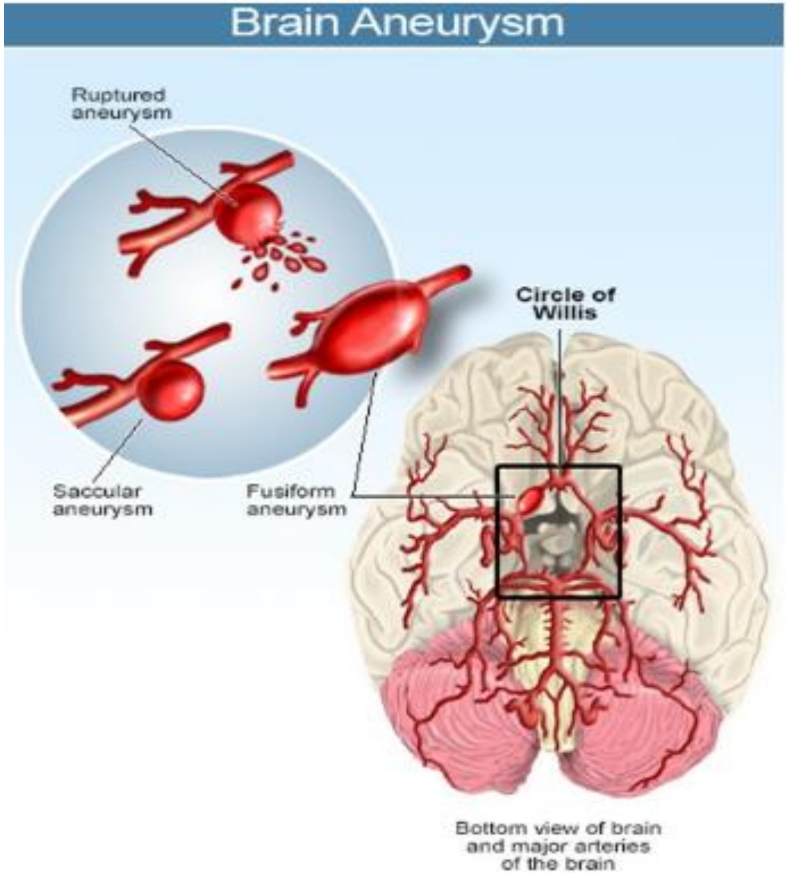

Figure1: Aneurysm and location of brain aneurysm. Source: MedicineNet.com

Intracranial Aneurysm

Sidewall Aneurysm:

- On the side of a blood vessel
- Treatment is challenging

Bifurcation Aneurysm:

- At the branching point (bifurcation) of blood vessels, where two arteries diverge

- Both diagnosis and treatment are challenging

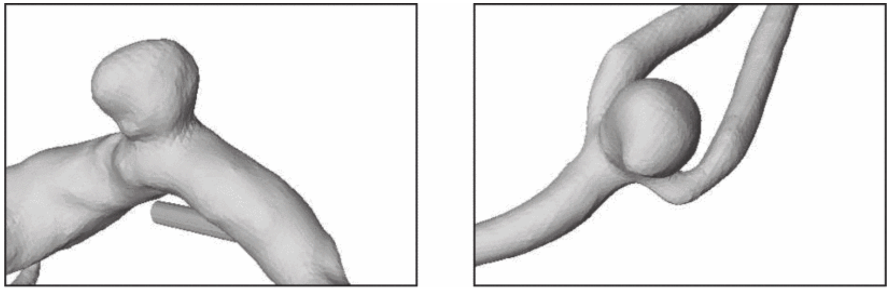

Figure2: Illustration of a sidewall aneurysm at the side of the parent vessel wall (left) and a bifurcation aneurysm at a vessel bifurcation (right).

Research Gap

Existing Literature

- Focused on patients with known rupture outcomes (Retrospective)
- Identifies common factors that were present in those cases
- Not real time or adaptive

Gap

- Dynamic, adaptive classification models for prediction (Going to rupture or not)
- Essential for clinicians to work with real-time patient-specific data

Objective

- Reduce risky treatments in case of low-risk aneurysms
- Feature Ranking: To find out which morphological features contribute most to rupture risk classification
- Compare performance between feature engineering and deep learning (learning on raw image data) in rupture risk assessment
- Propose a supervised learning based pipeline focused on sidewall and bifurcation aneurysm types

Methodology

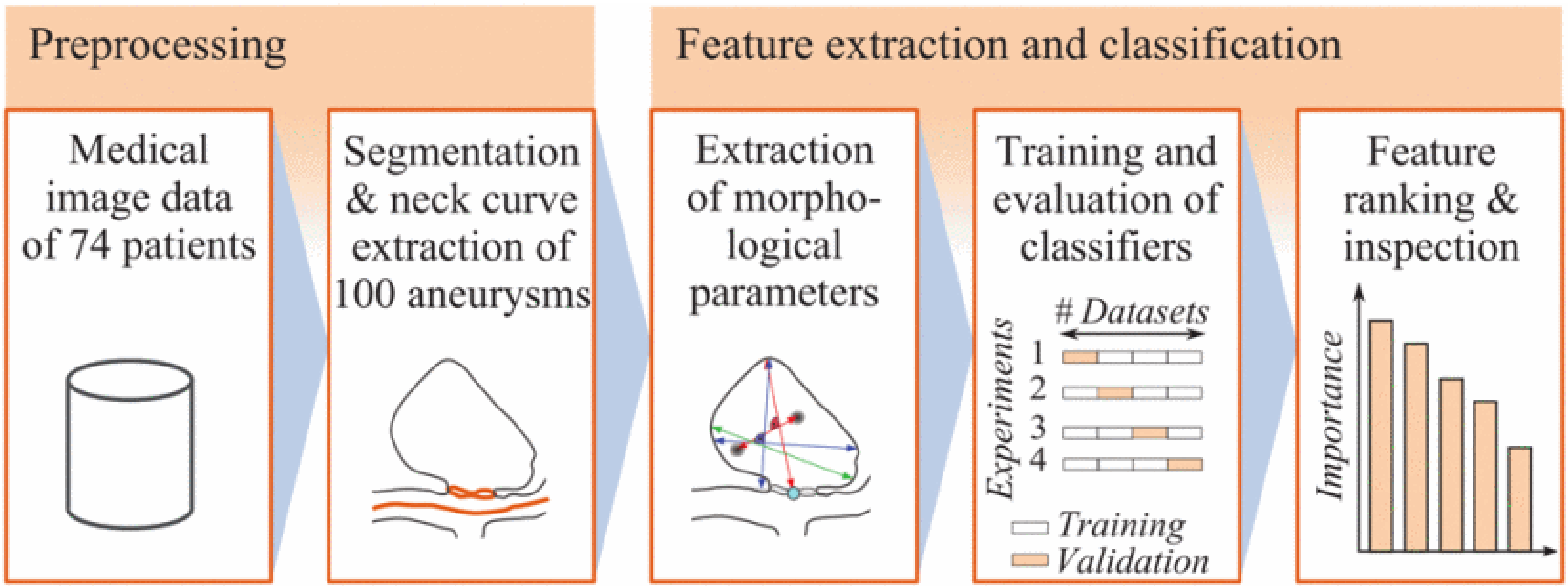

Figure3: Pipeline: data acquisition -> segmentation, neck curve extraction-> extraction of morphological features -> classification, evaluation-> feature ranking

Methodology

Extraction of morphological features

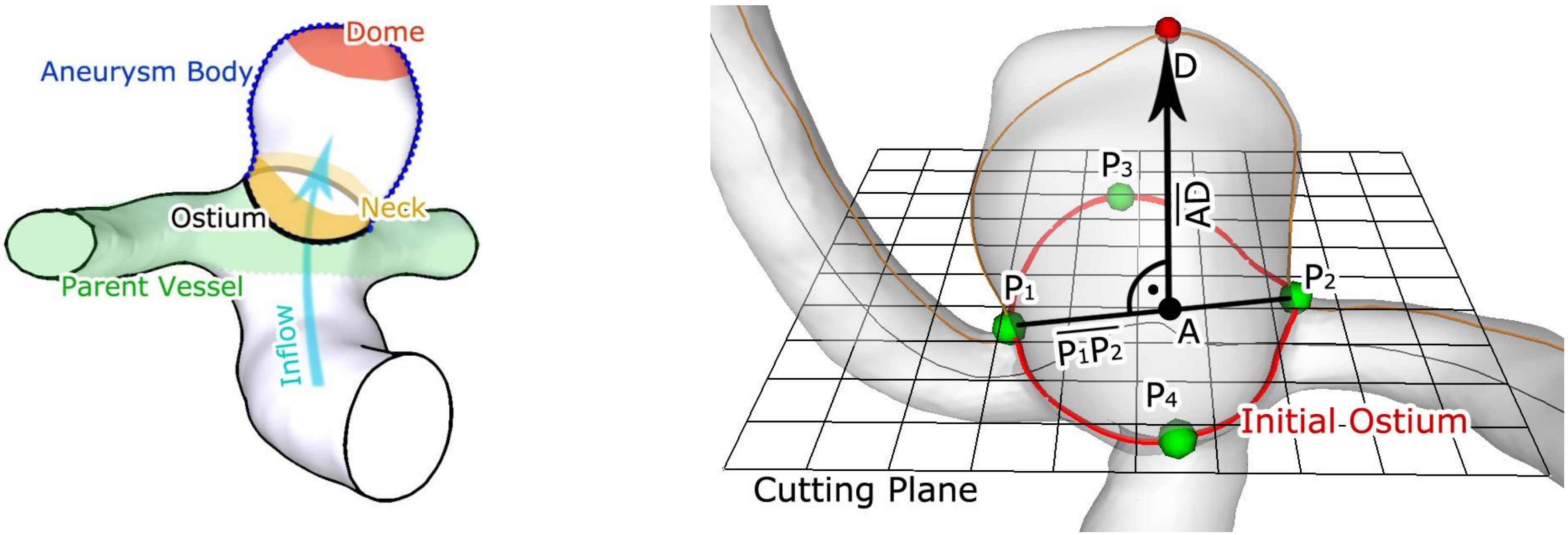

Figure 4: **Left**: The ostium seperates the aneurysm body from the parent vessel. The aneurysm body can be decomposed into neck and dome. **Right**: The initial ostium is constructed by cutting the surface with a plane that has AD as normal vector.

Image Reference: Neugebauer, Mathias & Diehl, Volker & Skalej, Martin & Preim, Bernhard. (2010). Geometric Reconstruction of the Ostium of Cerebral Aneurysms.. VMV 2010 - Vision, Modeling and Visualization. 307-314. 10.2312/PE/VMV/VMV10/307-314.

Methodology: extracting features

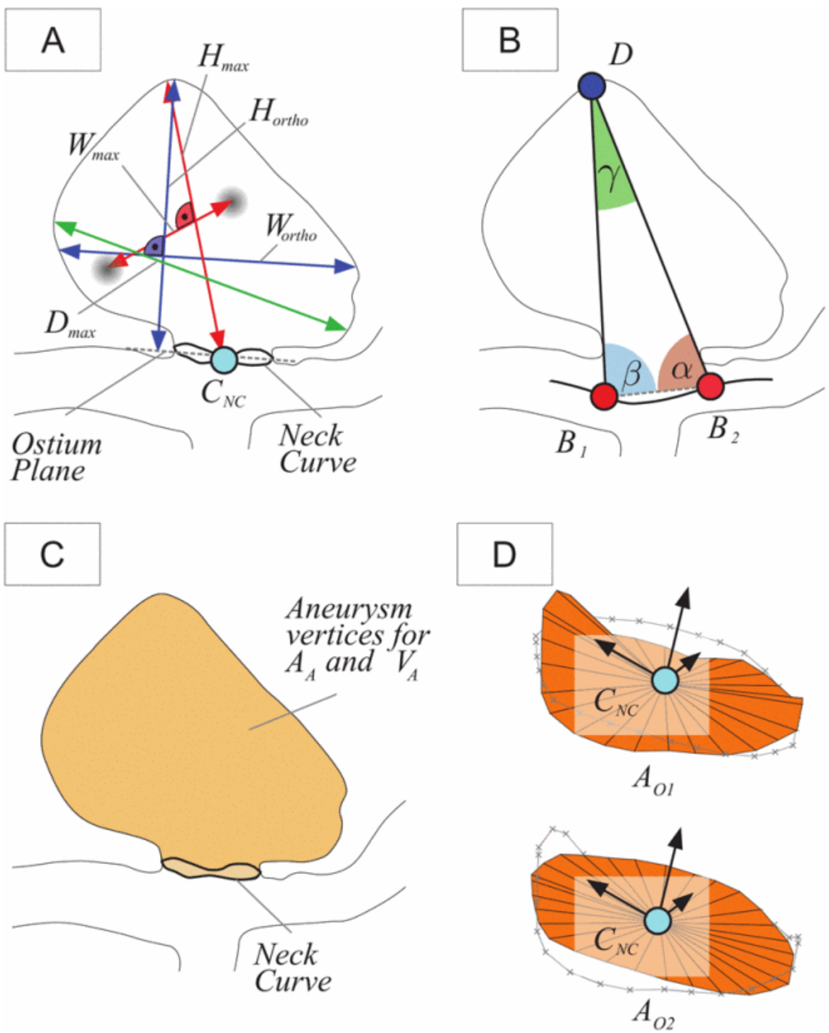

N_{max}	Max. NC diameter, i.e., the max. possible distance between two NC points $[mm]$
N_{avg}	Avg. NC diameter, i.e., the mean distance between C_{NC} and the NC points $[mm]$
β	Max. of $\measuredangle DB_1B_2$ and $\measuredangle DB_2B_1$ $[deg]$
γ	Angle at D, i.e. $\measuredangle B_1DB_2$ $[deg]$
D_{max}	Max. diameter of the aneurysm $[mm]$
H_{max}	Max. height of the aneurysm $[mm]$
W_{max}	Max. width of the aneurysm perpendicular to H_{max} $[mm]$
H_{ortho}	Height of the aneurysm approximated as length of the ray perpendicular to the ostium plane starting from C_{NC} $[mm]$

Figure5. Illustration of the extracted morphological features Hmax, Wmax, Hortho, Wortho and Dmax (A). The angles , and are extracted based on B1, B2 and the dome point D (B). Separating the aneurysm from the parent vessel based on the neck curve yields AA and VA (C). The area of the ostium and the projected ostium, i.e., AO1 and AO2, are shown in (D), where CNC denotes the center of the neck curve.

Methodology: Extraction of features

- Aspect ratios and angle at dome point → Correlation with very high confidence.

Description	Status	$\bar{x} \pm s$	Distribution	p-value
Aspect ratio: H_{ortho}/N_{max}	Unruptured Ruptured	1.08 ± 0.50 1.40 ± 0.56	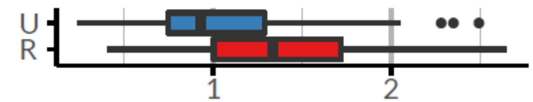	**0.002****
Aspect ratio: H_{ortho}/N_{avg}	Unruptured Ruptured	1.23 ± 0.56 1.60 ± 0.65	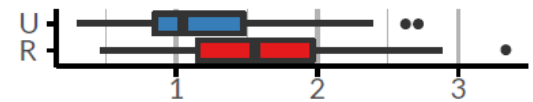	**0.003****
Max. of $\measuredangle DB_1B_2$ and $\measuredangle DB_2B_1$ $[deg]$	Unruptured Ruptured	80.70 ± 17.07 92.13 ± 17.29	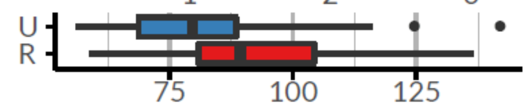	$<$**0.001****
Angle at D, i.e. $\measuredangle B_1DB_2$ $[deg]$	Unruptured Ruptured	44.93 ± 19.71 30.98 ± 13.68	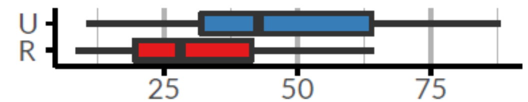	$<$**0.001****

Figure6: Morphological features used for classification, with mean values and standard deviation . boxplots provide summaries of the feature distributions for unruptured (u) and ruptured (r) aneurysms. p-values were derived from a statistical analysisusing the non-parametric mann-whitney-u test; significant correlation (double-sided) with p < 0.01; significant correlation (double-sided) with p < 0.05

Methodology: Extraction of features

- Features related to size (e.g., maximum height, diameter) -> Correlation with high confidence.

Description	Status	$\bar{x} \pm s$	Distribution	p-value
Height of the aneurysm approximated as length of the ray perpendicular to the ostium plane starting from C_{NC} $[mm]$	Unruptured Ruptured	4.26 ± 2.41 5.17 ± 2.41	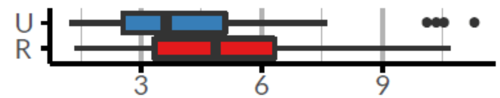	**0.030***
Max. diameter of the aneurysm $[mm]$	Unruptured Ruptured	6.24 ± 2.84 7.21 ± 2.77	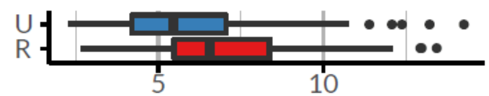	**0.034***
Max. height of the aneurysm $[mm]$	Unruptured Ruptured	4.74 ± 2.54 5.88 ± 2.59	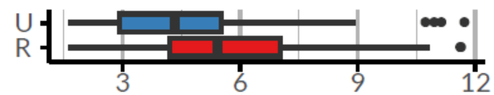	**0.012***

Figure7: Morphological features used for classification, with mean values and standard deviation . boxplots provide summaries of the feature distributions for unruptured (u) and ruptured (r) aneurysms. p-values were derived from a statistical analysisusing the non-parametric mann-whitney-u test; significant correlation (double-sided) with $p < 0.01$; significant correlation (double-sided) with $p < 0.05$

Methodology: Classification

- (100 sample images + 22 morphological feature input features) -> Model -> Two class target feature (Ruptured / Unruptured)

- 10 algorithms deployed for classification

- Transformations:

Range: Makes variables comparable , prevents issues due to varying scales,
Z-score: Centers the data around zero and scales it based on its variability,
PCA : Reduces high dimensionality. Only the first principal components ->capturing majority of the data's variability.

- 5 times repeated 10-fold Stratified Cross-validation:

-> A total of 50 model evaluations (5 repetitions * 10 folds)
-> Each instance in the original dataset has been part of the test set exactly once
-> Ensures that the class distribution in each fold is representative of the overall dataset

Results

Subset	Algorithm	Prepr.	Acc.	Kappa	AUC
ALL	GBT	-	.69±.15	.36±.32	.70±.02
	C5.0	-	.66±.16	.32±.31	.68±.04
	GPLS	-	.66±.15	.28±.31	.69±.01
	KNN	range	.66±.16	.27±.34	.63±.01
	CART	-	.65±.12	.29±.26	.61±.03
	NNET	range	.62±.13	.23±.26	.64±.03
	C4.5	-	.62±.15	.24±.31	.64±.03
	NBayes	-	.61±.16	.21±.32	.58±.03
	SVMLin	-	.60±.15	.17±.32	.56±.02
	RF	-	.60±.12	.16±.26	.62±.01
SW	SVMLin	-	.80±.24	.50±.53	.66±.12
	GPLS	range	.79±.26	.49±.56	.73±.03
	C5.0	-	.78±.30	.50±.60	.83±.03
	KNN	pca	.77±.21	.38±.49	.73±.04
	GBT	-	.77±.27	.49±.55	.68±.03
	NNET	range	.75±.28	.42±.58	.69±.05
	CART	-	.75±.34	.47±.66	.63±.06
	RF	-	.74±.28	.40±.55	.69±.05
	NBayes	-	.72±.32	.45±.59	.68±.03
	C4.5	-	.72±.32	.40±.61	.75±.06
BF	GPLS	center, scale	.68±.16	.34±.32	.68±.02
	KNN	pca	.66±.19	.33±.38	.68±.02
	NNET	center, scale	.63±.18	.25±.37	.65±.02
	SVMLin	-	.63±.17	.26±.33	.62±.04
	GBT	-	.62±.15	.24±.29	.59±.04
	NBayes	-	.61±.19	.24±.37	.57±.03
	CART	-	.61±.18	.22±.34	.61±.04
	C4.5	-	.60±.15	.21±.29	.62±.03
	RF	-	.60±.16	.19±.32	.63±.02
	C5.0	-	.59±.16	.19±.32	.61±.02

Table1: classification performance for each combination of data subset and algorithm

- No single classification algorithms outperforms all others across all subsets.

- **All (sidewall + bifurcated+ unknown)**:

- GBT performs best with an accuracy of 69%.
- C5.0, GPLS, and KNN follow closely, each achieving 66% accuracy.

- **Sidewall (SW) Subset**:

- SVMLin with a range transformation achieves the highest accuracy at 80%.
- GBT, C5.0, GPLS, and KNN also exhibit improved performance on the SW subset.

- **Bifurcated (BF) Subset**:

- GPLS with a z-score transformation performs best, achieving 68% accuracy and an AUC of 0.68.

Results

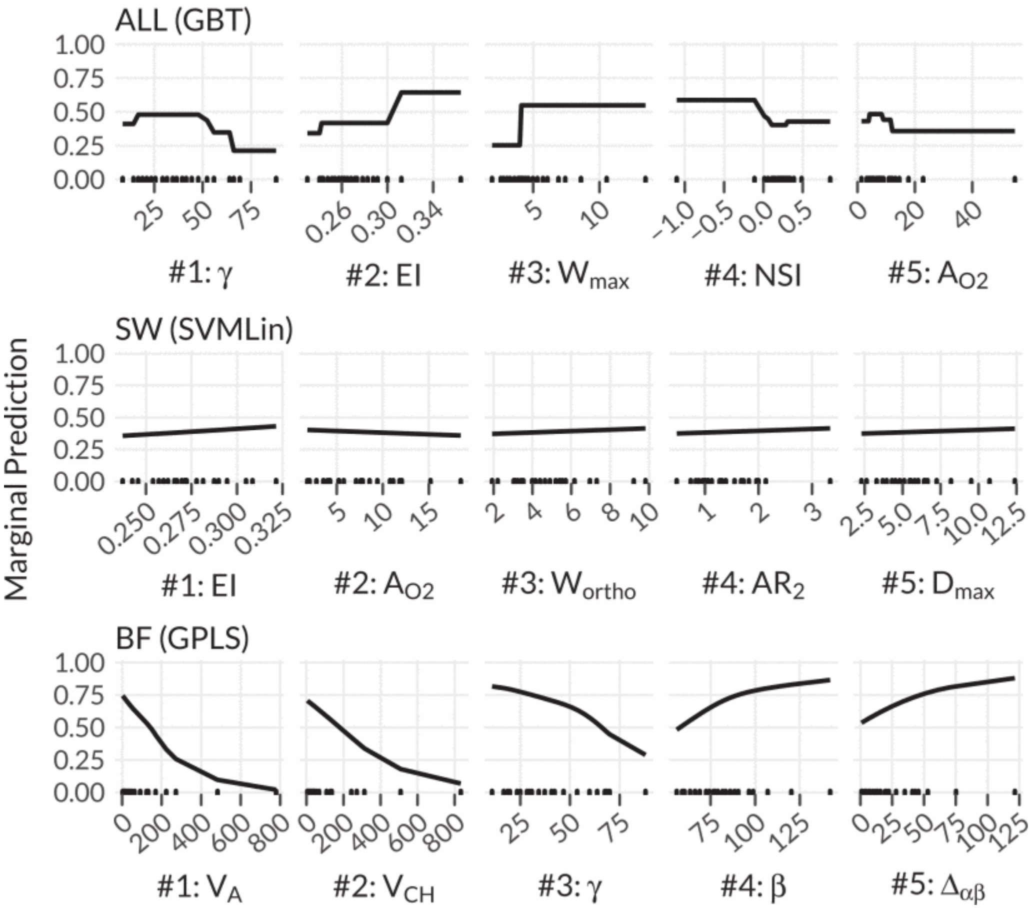

Figure8: The partial dependence plots show the marginal prediction of the five most important variables for the best model of each data subset

- Angle at dome is crucial in rupture status classification
- The lower the angle values, the higher the likelihood of ruptured aneurysms.

TECHNISCHE UNIVERSITÄT ILMENAU

Results

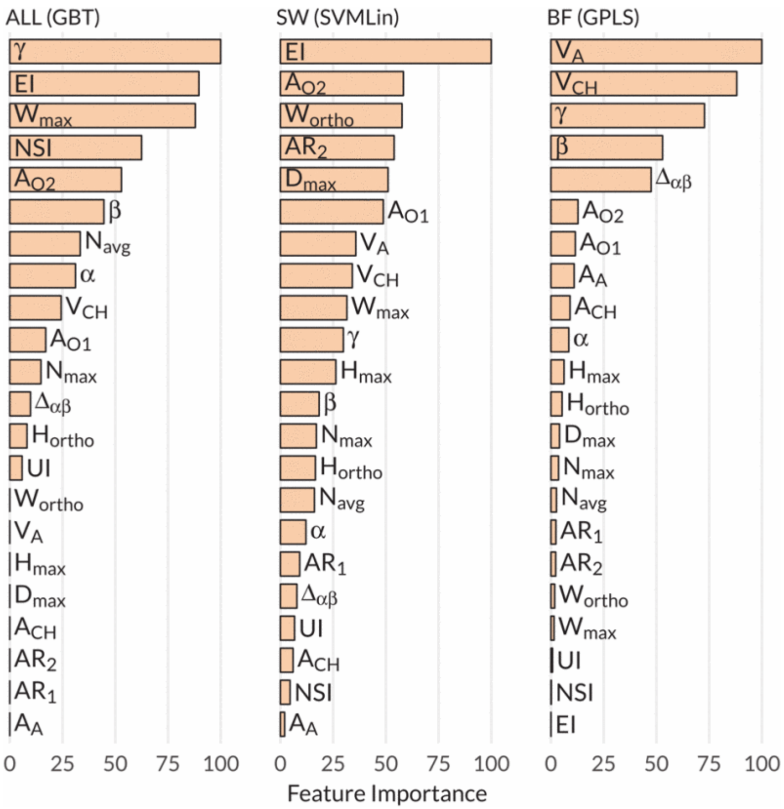

Figure9: Feature importance for the best model of each data subset. Values are scaled up to 100 according to the highest feature importance.

EI	Ellipticity index: $1-(18\pi)^{\frac{1}{3}}\, V_{CH}^{\frac{2}{3}}/A_{CH}$	Unruptured	0.27 ± 0.02
		Ruptured	0.27 ± 0.02

- Mean and standard deviation of ellipticity index (EI) are same for ruptured and unruptured.
- Still, most important in sidewall and 2nd most important in ALL ! How ?
- Gets combined with other features by the model at the time of prediction
- Indicates interdependencies between input features.

TECHNISCHE UNIVERSITÄT ILMENAU

Results

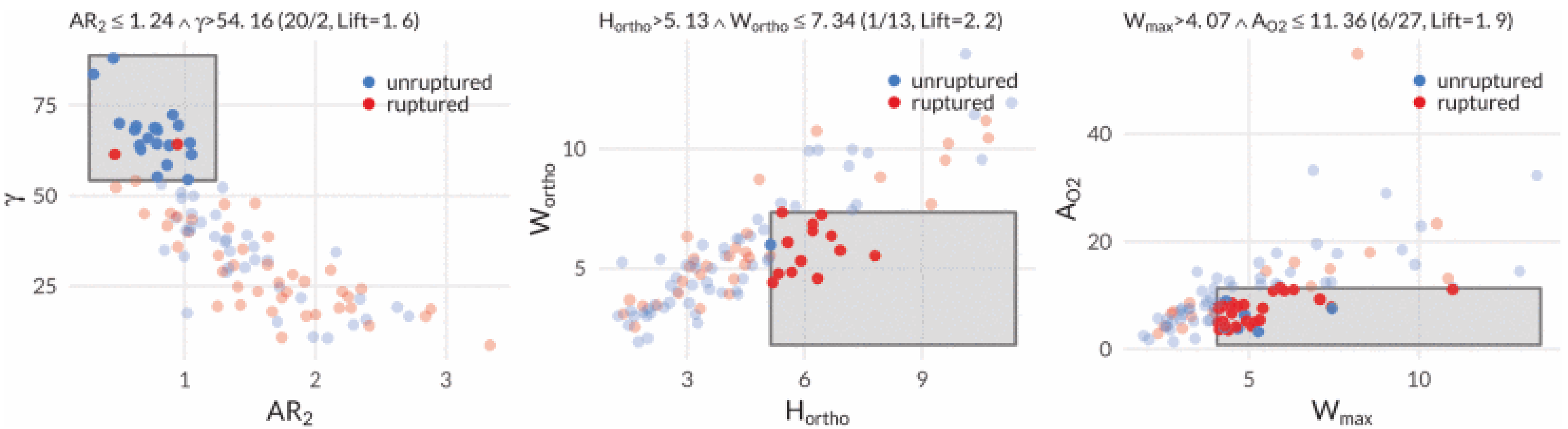

Figure9: Three classification rules with high lift values extracted from C5.0 for subset ALL. The title of a subfigure displays the rule's condition. The class counts and lift value of the partition are given in parenthesis. Samples that satisfy the rule condition are shown as opaque points within a gray box.

- Lift 1.6 -> within the partition by the rule, the relative frequency of the class "unruptured" is 1.6 times higher than in the total training set

TECHNISCHE UNIVERSITÄT ILMENAU

Results

- Majority class prediction yields 57% accuracy, outperforming single-feature classifier (55%),

- Indicates limited predictive power of individual features,

- Emphasizes the necessity for more advanced models or feature combinations in aneurysm rupture status classification

Limitations

- Limited sample size, especially for sidewall aneurysms
- Potential over-fitting of classification models due to the small dataset
- Quality of class labels might be impacted by the dynamic nature of aneurysm pathology
- Overlooking other potentially predictive properties like hemodynamic (related to blood flow dynamics in vessels) features

Future Work

- Evaluate model robustness on larger datasets,
- Investigate samples with high classification errors to understand reasons for misclassification.
- Quantify the impact of careful feature engineering compared to models learned on raw image data (Deep Learning).
- Consider incorporating a broader range of feature types to enhance model accuracy.

References and acknowledgement

[1] U. Niemann et al., "Rupture Status Classification of Intracranial Aneurysms Using Morphological Parameters," 2018 IEEE 31st International Symposium on Computer-Based Medical Systems (CBMS), Karlstad, Sweden, 2018, pp. 48-53, doi: 10.1109/CBMS.2018.00016.

[2] An interactive web application available at https://rbsenzaehler.shinyapps.io/RUSTiC/

[3] Jersey AM, Foster DM. Cerebral Aneurysm. [Updated 2023 Apr 3]. In: StatPearls [Internet]. Treasure Island (FL): StatPearls Publishing; 2023 Jan-. Available from: https://www.ncbi.nlm.nih.gov/books/NBK507902/

This work was partially funded by the German Federal Ministry of Education and Research within the Research Campus STIMULATE (grant number ‘13GW0095A’).

Thank you

for your attention .

Any questions ?